SAE International

Comparison of Calculated Speeds for a Yawing and Braking Vehicle to Full-Scale Vehicle Tests

2012-01-0620
Published
04/16/2012

Neal Carter, Gray Beauchamp and Nathan A. Rose
Kineticorp LLC

Copyright © 2012 SAE International
doi:10.4271/2012-01-0620

ABSTRACT

Accurately reconstructing the speed of a yawing and braking vehicle requires an estimate of the varying rates at which the vehicle decelerated. This paper explores the accuracy of several approaches to making this calculation. The first approach uses the Bakker-Nyborg-Pacejka (BNP) tire force model in conjunction with the Nicolas-Comstock-Brach (NCB) combined tire force equations to calculate a yawing and braking vehicle's deceleration rate. Application of this model in a crash reconstruction context will typically require the use of generic tire model parameters, and so, the research in this paper explored the accuracy of using such generic parameters. The paper then examines a simpler equation for calculating a yawing and braking vehicle's deceleration rate which was proposed by Martinez and Schlueter in a 1996 paper. It is demonstrated that this equation exhibits physically unrealistic behavior that precludes it from being used to accurately determine a vehicle's deceleration rate. Finally, the paper moves on to consider an equation that is attributed to the CRASH program in the 2010 edition of Traffic Crash Reconstruction by Lynn Fricke. This equation is nearly as simple as the Martinez and Schlueter equation, but its behavior is more reasonable.

The BNP/NCB and the CRASH models are then used to calculate vehicle deceleration rates and speeds for two full-scale vehicle tests run by the authors, both involving yawing and braking vehicles. Braking levels for the vehicles in these tests were calculated using analysis of tire mark striations. The results of these speed calculations are compared to the measured speeds for each of those full-scale tests.

INTRODUCTION

Mathematically predicting the motion of a vehicle in response to driver steering and braking inputs requires calculation of the resultant tire force at each wheel position. Vehicle dynamics simulation programs use such an approach to calculate vehicle linear and rotational motion. However, in a crash reconstruction context, simulation is not always necessary, and a more simple analysis can yield the rate at which a vehicle decelerated due to tire forces along a known path. In this paper, the primary goal will be to calculate a yawing and braking vehicle's translational speed at the beginning of tire mark evidence using a calculated deceleration rate. Three models were considered and will be discussed below.

BAKKER-NYBORG-PACEJKA (BNP) AND NICOLAS-COMSTOCK-BRACH (NCB) MODEL

This tire modeling method begins by modeling and calculating normalized longitudinal and lateral tire forces as if they could be decoupled, calculating each one as if the other was not present. In other words, the actual braking (or longitudinal slip) level will be used to calculate a normalized longitudinal tire force component as if there was no sideslip angle. Then, the actual tire sideslip angle will be used to calculate a normalized lateral tire force component as if there was no braking. These calculations are carried out using a zero-sideslip angle longitudinal tire force curve and a free-rolling lateral tire force curve generated using generic, representative coefficient values with the "magic formula" of Bakker, Nyborg and Pacejka, or the BNP model [Reference 1]. These BNP model equations are used to calculate decoupled normalized longitudinal and lateral tire forces as a function of the longitudinal wheel slip ratio (s) and

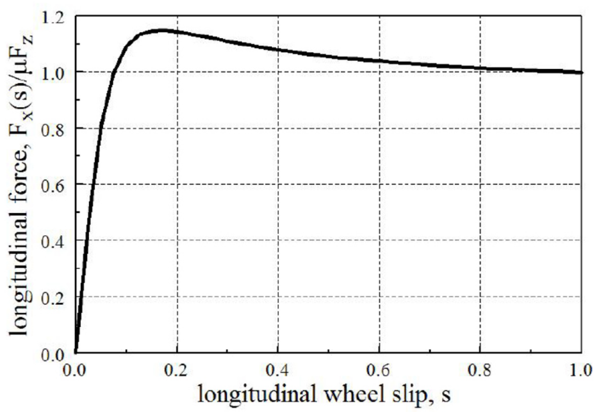

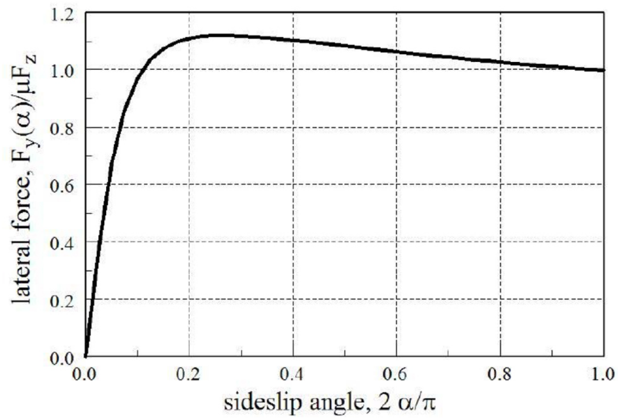

Figure 1. Representative Normalized Longitudinal and Lateral Tire Force Curves

normalized tire sideslip angle *($2\alpha/\pi$)*, respectively (α is the tire sideslip angle, in radians).

For the analysis carried out in this paper, there will not be any need to calculate the actual magnitude of the tire forces. Instead, the calculations will yield tire forces that have been normalized with the normal load on the tire. We will use the letter Q to refer to the normalized tire forces in order to distinguish them from the actual tire force magnitudes, for which the literature typically uses the letter *F*. The generic functional form of the BNP model equations for the normalized tire forces is shown below in Equation (1). Both the lateral and longitudinal tire force equations will take this form, and so we have written this equation without any subscripts on the Q and with a generic slip ratio, *u*. When modeling longitudinal tire forces, the generic argument *u* will become the longitudinal slip ratio, *s*. When modeling lateral tire forces, *u* will become the lateral sideslip ratio, $2\alpha/\pi$ (this could also be referred to as the normalized sideslip angle).

$$Q(u) = D\ \sin\{C \tan^{-1}[B\ (1-E)Ku + E\ \tan^{-1}(BKu)]\} \tag{1}$$

When using this function to model the normalized longitudinal tire force, $Q_x(s)$, the longitudinal slip ratio of the tire, *s*, can vary between zero and one. A value of zero corresponds to a free rolling tire and a value of one corresponds to a fully locked tire. Similarly, for the normalized lateral tire force, $Q_y(2\alpha/\pi)$, the lateral sideslip ratio or normalized tire sideslip angle can vary between zero and one. A value of zero corresponds to a sideslip angle of zero and a value of one corresponds to a sideslip angle of 90 degrees.

The parameter *K* in Equation (1) is set to a value of 100 and acts as a scaling value to convert the lateral and longitudinal slip ratios to percentages. The coefficients *B*, *C*, *D*, and *E* are shape parameters that are chosen to empirically model a specific set of tire data. For the calculations described in this paper, the authors chose shape parameters that would yield typical or representative tire force curves. Specifically, we chose to match the curves shown in Figure 1 below, which are from Reference 4 by Brach and Brach. The graph on the left below represents the normalized longitudinal tire force plotted with respect to the longitudinal slip ratio for a zero sideslip angle. The graph on the right represents the normalized lateral tire force plotted with respect to the lateral sideslip ratio or normalized slip angle for a longitudinal slip of zero. Table 1 lists the coefficients used in Equation (1) to match the curves depicted in each of these graphs.

Table 1. Coefficient Values for Lateral and Longitudinal BNP Equations

Parameter	Value for Longitudinal Tire Force Curve	Value for Lateral Tire Force Curve
B	0.118	0.093
C	1.398	1.498
D	1.152	1.124
E	-0.128	0.573

The curves of Figure 1 assume either yawing with no braking or braking with no yawing. For a vehicle undergoing both yawing and braking, the magnitudes of the longitudinal and lateral components of the tire force cannot be decoupled in this way. Braking will reduce the force available for cornering, for instance. In terms of calculating an actual resultant tire force, this situation could be remedied by generating numerous tire force curves with Equation (1), longitudinal tire force curves for a number of sideslip angle conditions and lateral tire force curves for a number of longitudinal slip levels. Values would then be selected from these curves or functions based on the actual lateral and longitudinal slip conditions. This is a rather cumbersome solution, though, particularly within a crash reconstruction context where these calculations would often be carried out within a spreadsheet. Additionally, each BNP function would require its own set of four coefficients, none of which would likely be known with any certainty for a crash reconstruction.

A simpler approach would be to combine the calculated decoupled longitudinal and lateral tire forces in a way that incorporates their interdependence and effect on one another. The Nicolas-Comstock-Brach (NCB) model provides such a method for combining decoupled longitudinal and lateral tire forces [References 2, 3, 4, and 5]. These equations are listed below.

$$Q_x(\alpha,s) = \frac{Q_x(s)Q_y(\alpha)}{\sqrt{s^2Q_y^2(\alpha)+Q_x^2(s)tan^2\alpha}} \cdot \frac{\sqrt{s^2C_\alpha^2+(1-s)^2cos^2\alpha Q_x^2(s)}}{C_\alpha} \tag{2}$$

$$Q_y(\alpha,s) = \frac{Q_x(s)Q_y(\alpha)}{\sqrt{s^2Q_y^2(\alpha)+Q_x^2(s)tan^2\alpha}} \cdot \frac{\sqrt{(1-s)^2cos^2\alpha Q_y^2(\alpha)+sin^2\alpha C_s^2}}{C_s cos\alpha} \tag{3}$$

C_s and C_α are determined from the coefficients in the BNP equations and are defined as follows:

$$C_s = (BCDK)_s \tag{4}$$

$$C_\alpha = (BCDK)_\alpha \tag{5}$$

Once the normalized components of the tire forces are calculated, an effective deceleration rate for each tire can be calculated with the following equation [Reference 3].

$$f_{eff,i} = \mu_0 \cdot \left[Q_x(\alpha,s)\cdot cos(\alpha) + Q_y(\alpha,s)\cdot sin(\alpha)\right] \tag{6}$$

This equation projects the tire force components onto the vehicle velocity direction to determine the portion of these tire forces that is opposing the velocity at any particular point, a concept that is illustrated from a top down view in Figure 2. In this equation, μ_0 is the nominal roadway coefficient of friction and $f_{eff,i}$ is the effective deceleration rate at the i^{th} wheel position. An effective deceleration rate should be calculated for each wheel position.

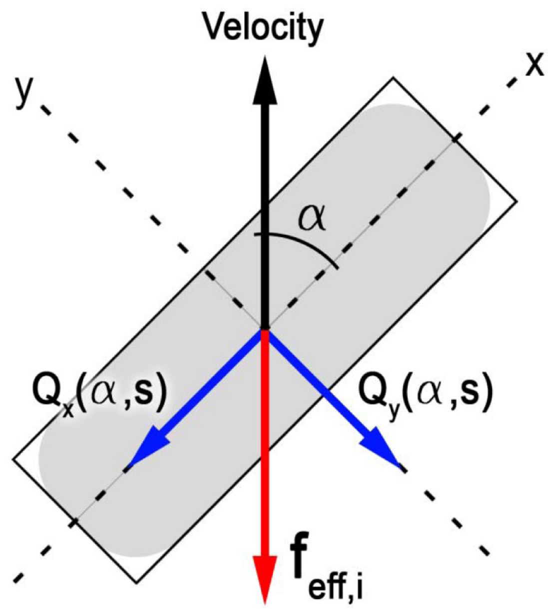

Figure 2. Direction of $f_{eff,i}$, $Q_X(\alpha,s)$, $Q_y(\alpha,s)$ in Relation to the Velocity Direction and α

Once an effective deceleration rate is obtained for each wheel position, they can be combined into an effective deceleration rate for the vehicle as a whole with the following equation. In this equation, W_{total} is the total weight of the vehicle, W_i is the static weight on each wheel position and N is the total number of wheels.

$$f_{veh} = \frac{1}{W_{total}}\sum_{i=1}^{N}\left[f_{eff,i}\cdot W_i\right] \tag{7}$$

Brach's papers have demonstrated that when combined, the BNP and NCB models can yield realistic tire force component calculations and vehicle motion for simulations with conditions of combined braking and cornering [References 2, 3, 4, and 5]. Later in this paper, we will verify that this accuracy translates from a forward-simulation context to a backwards-reconstruction context (where the motion is known from physical evidence and the forces that caused that motion are being inferred). Specifically, we will verify that the BNP and NCB models can be used with typical or representative parameters to obtain accurate vehicle speeds for a braking and cornering vehicle with Equations (6) and (7).

MARTINEZ-SCHLUETER MODEL

In Reference 6, Martinez and Schlueter proposed the following equation for calculating the deceleration rate of a vehicle undergoing both yawing and braking:[1]

[1] Reference 7 contains additional discussion of this equation.

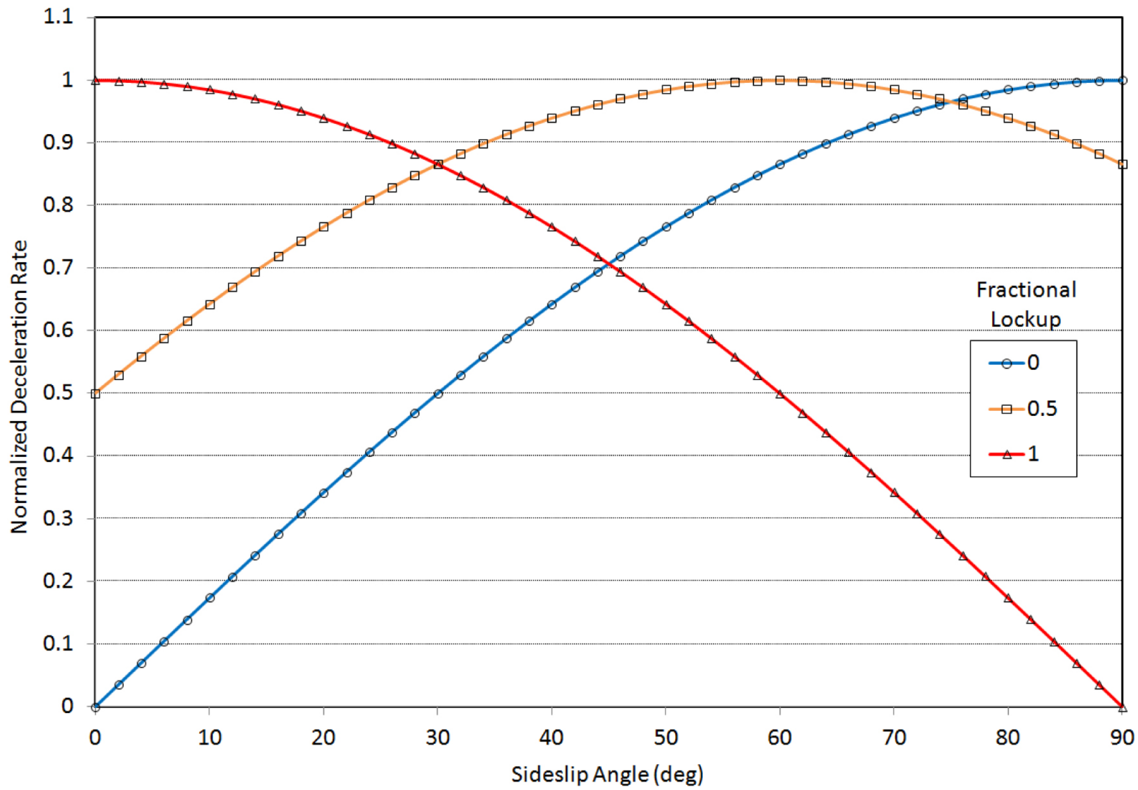

Figure 3. Result of Martinez Equation for Various Sideslip Angles and Fractional Lockup Values

$$f_{veh} = \mu_0 \sin\left[\alpha + \tan^{-1}\left(\frac{\kappa_B}{\sqrt{1-\kappa_B^2}}\right)\right] \tag{8}$$

In this equation, κ_B is a parameter Martinez and Schlueter termed "fractional lockup." This term is not defined in their paper, but we presume it was intended to equal the braking level as a proportion of the available friction, and having values ranging from zero to one. This model displays physically unrealistic behavior. As an example, consider a vehicle with a sideslip angle of 90 degrees. At this sideslip angle, the deceleration rate of the vehicle should be equal to the nominal friction coefficient, independent of the level of braking. However, for a 90 degree sideslip angle and a fractional lockup of 0.5, Equation (8) yields a deceleration rate of $0.866\mu_0$. The deceleration rate continues to decline as the braking level increases, approaching zero as the fractional lockup approaches 1.0 (locked-wheel braking).

Examination of the bracketed terms in Equation (8) reveals the source of this error. As κ_B approaches a value of 1.0 (locked-wheel braking), the inverse tangent term approaches 90 degrees. When this angle is combined with the sideslip angle, the result is a term that can vary between 0 and 180 degrees. This model deviates from the expected behavior because the sine function decreases for angles greater than 90 degrees. The graph below (Figure 3) depicts this incorrect behavior of Equation (8) across a wider range of conditions. It presents the normalized deceleration (the deceleration rate divided by the sliding friction) calculated from the Martinez equation for various values of κ_B and α.

The curve for a fractional lockup of zero exhibits reasonable behavior. Once braking is added, however, the behavior of the model degrades significantly. With a fractional lockup of 0.5, the curve begins at 0.5, as it should. It then rises to a peak of 1.0 at a sideslip angle around 60 degrees - reasonable behavior. Beyond that point, however, the behavior of the model becomes unrealistic, with the deceleration rate decreasing with increasing sideslip angle. In actuality, the deceleration rate should remain near 1.0 through the range of sideslip angles from 60 to 90 degrees. The behavior of the curve with a fractional lockup of 1.0 is worse. It should exhibit a deceleration rate near 1.0 across the entire range of sideslip angles. Instead, it starts at a normalized deceleration rate of 1.0 and steadily diminishes to zero across the range of sideslip angles from 0 to 90 degrees. The unrealistic behavior of Equation (8) led us to reject its use for the remainder of this research.

CRASH MODEL

Another option for calculating a yawing and braking vehicle's deceleration rate is included in the 2010 edition of Traffic

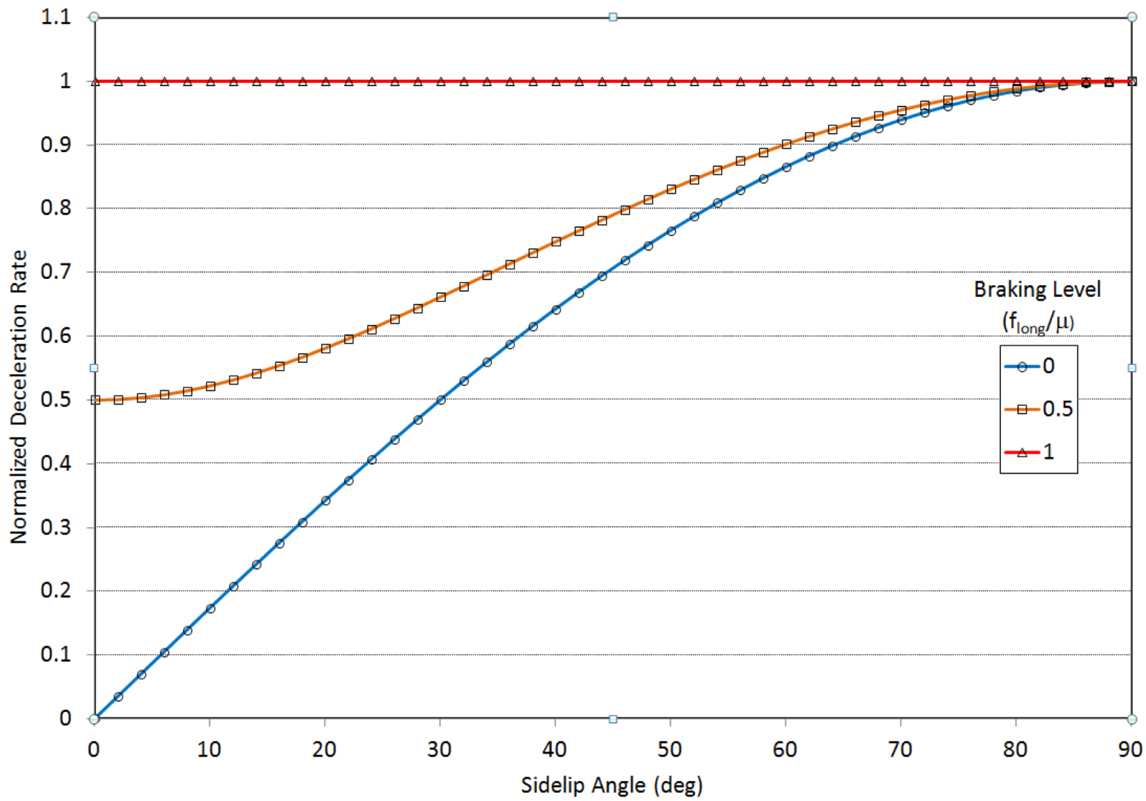

Figure 4. Result of CRASH Equation for Various Sideslip Angles and Braking Levels

Crash Reconstruction by Lynn Fricke [Reference 8]. This equation, which Fricke attributed to the CRASH program, is listed below:

$$f_{veh} = \mu_0 \sqrt{sin^2\alpha + \left(\frac{f_{long}}{\mu_0}\right)^2 cos^2(\alpha)} \qquad (9)$$

The behavior and physical accuracy of this equation is significantly better than that of Equation (8). Sample curves plotted using this equation are included in Figure 4 below. In this graph, the normalized deceleration rate is plotted as a function of sideslip angle and braking level. As this graph shows, Equation (9) yields a normalized deceleration rate of 1.0 for a braking level of 1.0, independent of the sideslip angle - physically correct behavior. For braking levels less than 1.0, the equation yields deceleration rates that start out at the braking level when the sideslip angle is zero and build up to 1.0 as the sideslip angle goes to 90 degrees, which is again physically reasonable behavior.

DESCRIPTION OF FULL SCALE TESTS

The authors conducted a number of yaw tests with a 2008 Chevrolet Malibu on August 18, 2008. Two of these tests will be considered here. The Malibu used for the testing was outfitted with Hankook Winter Ipike tires of size 225/60R16. The vehicle was instrumented with a VBOX IISX + Slip, Pitch and Roll Angle data acquisition system from Racelogic. The VBOX recorded the vehicle's translational and angular position and the Vehicle CAN Interface recorded wheel speeds and steering position from the Malibu's internal sensors. All data was recorded at 20 Hz. Figure 5 depicts the Malibu test vehicle with the three VBOX GPS antenna attached magnetically to its roof. The series of photographs in Figure 6 below were taken during yaw Test #2 and depicts motion typical of the tests. In addition to these tests, a straight-line skid-to-stop test was run to quantify the roadway coefficient of friction for the analysis reported later in this paper. For this test, the ABS system was disabled to allow for fully locked wheels during the deceleration. This test yielded a sliding friction value of 0.79.

Test 1: In the first test considered here, the Malibu was accelerated to a speed of approximately 48 mph. During our testing with the Malibu, several attempts were made to induce a yaw using only steering inputs. Although tracking of the rear tires outside the front tires did occur during these attempts, the yawing was insufficient to reach large sideslip angles. In order to induce yaw rotation of the magnitude needed for this study, the parking brake was applied temporarily to initiate the yaw. In this first test, the driver applied the parking brake and made a steering input to the left to induce severe yaw rotation. Once the yaw was initiated, the

Figure 5. Chevrolet Malibu Test Vehicle

Figure 6. Photographs Taken During Yaw Test #2

driver released the parking brake and the vehicle yawed approximately 180 degrees in a counter-clockwise direction. Once the parking brake was released, the driver reported no additional braking. The wheel speed sensor data, though, indicated there may have been some small amount of braking near the end of the test, when the vehicle was rolling backwards to rest.

The position of the test vehicle was documented before and after the test. The test surface was surveyed and photographed as were tire marks that the test vehicle deposited during the test. A scene diagram was created from this survey data. The data acquired with the VBOX was synchronized to the physical evidence (the tire marks) by importing both the scene diagram and the VBOX data into an animation software package. The VBOX data was assigned to a vehicle model within that animation software package and the motion of this vehicle was aligned to the tire marks. Once synchronized in this manner, the VBOX data could be examined at each vehicle location of interest.

The tire marks were analyzed to obtain inputs for our deceleration rate calculations. Specifically, we obtained the longitudinal slip percentage and sideslip angle for each of the vehicle's tires at a number of positions along the vehicle's path. At each selected position, the sideslip angles of the rear tires were determined based on the alignment of the vehicle with the tire marks. Since the front tires are steerable, the sideslip angles of the front tires were determined by adding or subtracting the steering angle at the tire from the sideslip angles at the rear tires. The longitudinal slip percentages of the Malibu tires were then calculated using striation analysis as presented in Reference 9. This reference presented equations that relate the orientation and spacing of yaw mark striations to the vehicle braking and steering levels present at the time the striations were deposited. Conceptually, such analysis relies on the idea that tire mark striations are direct physical evidence of the actual direction of the force that was applied to the tire at the time the mark was deposited. Without braking, the tire force is perpendicular to the tire heading, and thus, the striations produced are perpendicular to the tire heading. Thus, in conducting our analysis, we were calculating the longitudinal slip level that would result in the actual tire force direction lying along the striation direction.

Test 2: In the second test considered here, the Malibu was again accelerated up to a speed of approximately 48 mph. The parking brake was then applied and the driver made a steering input to the right initiating a clockwise yaw. The parking brake was then released and the driver applied the

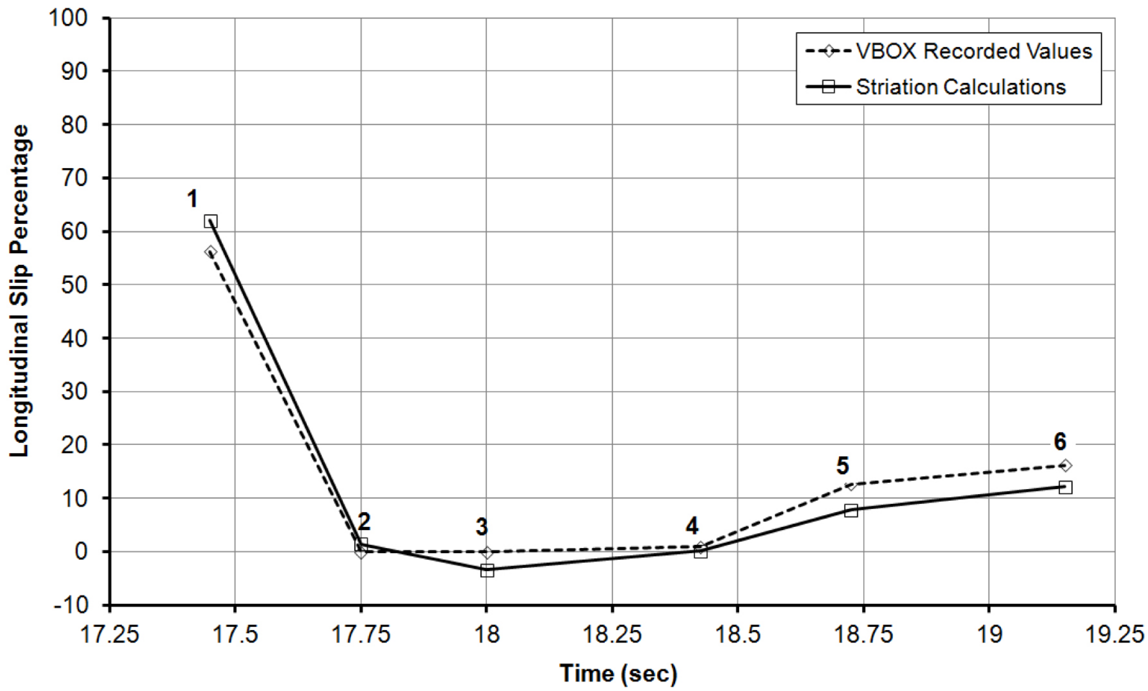

Figure 7. Calculated and Measured Longitudinal Slip Percentages for Test 2 Positions

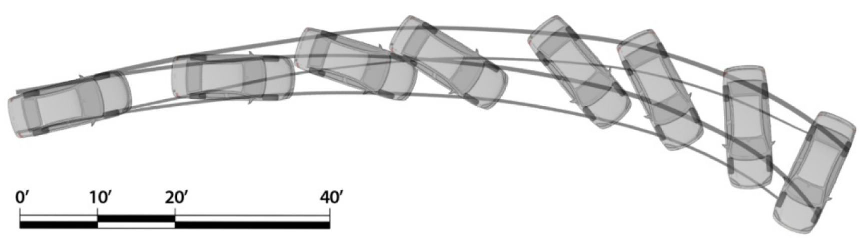

Figure 8. Analyzed Positions for Test 1

service brakes and counter-steered aggressively to the left. During the event, the vehicle yawed approximately 90 degrees. The wheel speed sensor data obtained from the VBOX showed that the ABS did not engage during the test.

Again, the position of the test vehicle was surveyed both before and after the test. The test surface and the tire marks that resulted from the test were surveyed and photographed. A scene diagram was created from this survey data and the data acquired with the VBOX was synchronized to the tire marks. The tire marks were analyzed to obtain inputs for our deceleration rate calculations. Some of the results of this tire mark analysis are shown in the graph below (Figure 7). This graph shows the longitudinal slip percentages for the left rear wheel. At the first position, the driver was in the process of releasing the parking brake (60% slip). The next three positions have longitudinal slip near 0% and represent the time between the release of the parking brake and application of the service brakes. Reflecting the service brake application, the slip percentage then increases to a value of around 10% for the 5th and 6th positions.

COMPARISON TO FULL SCALE TESTING

For each of these full-scale yaw tests, the authors conducted a speed analysis using two of the models discussed earlier, the BNP/NCB model and CRASH model. Also, a simple model that assumed no braking and another that assumed full wheel lockup were included for comparison. Using diagrams created from our site survey, vehicle models were aligned with the tire mark evidence as depicted in Figures 8 and 9. The segment lengths between positions were measured and the average vehicle sideslip angles were calculated based on the angles at the beginning and end of the segments. To account for braking, the BNP/NCB and CRASH models require the longitudinal slip percentages to be known. Tire mark striations were used to calculate longitudinal slip percentages [Reference 9].

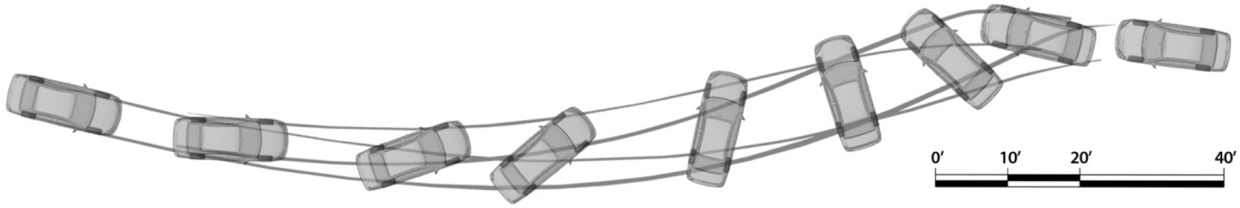

Figure 9. Analyzed Positions for Test 2

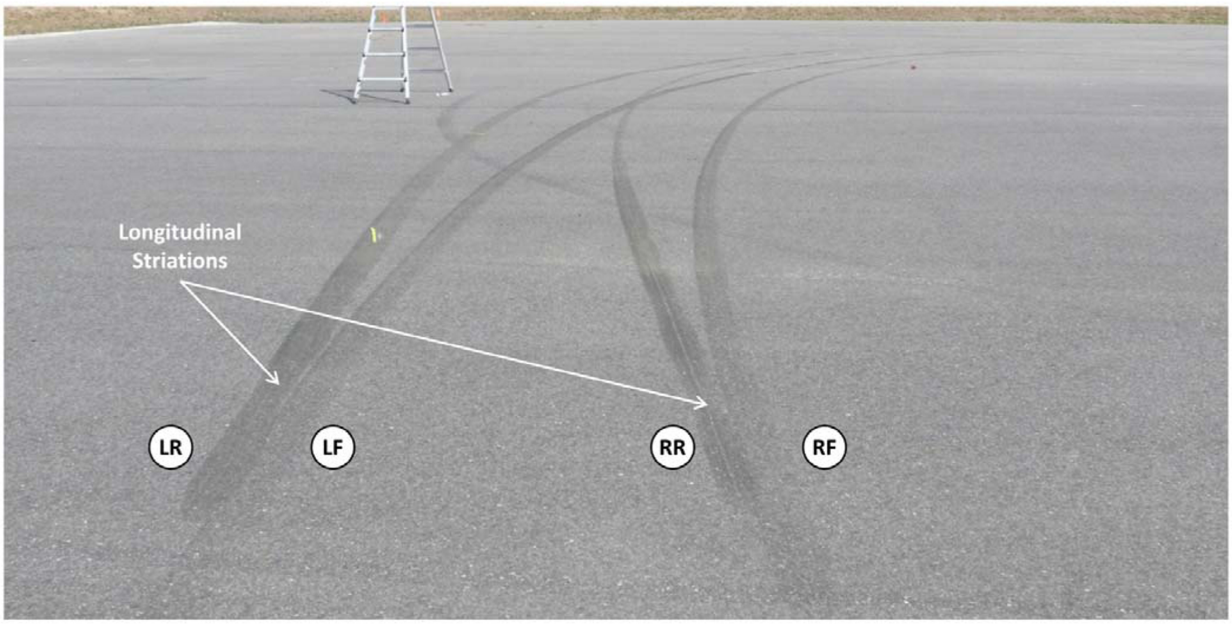

Figure 10. Tire Evidence Showing the Rear Tires Locked up in Test 2

During the phase of the yaws where the parking brake was applied, the rear tires of the Malibu locked while the front tires were unaffected. This lockup was apparent in the tire mark evidence. Figure 10, for instance, shows the tire marks from Test 2. In this figure, each tire mark has been labeled with the tire responsible for depositing it. Longitudinal striations indicating wheel lockup are evident in the early portions of the left and right rear tire marks. Thus, the longitudinal slip percentage of the rear tires were assigned a value of 100% during this phase. Lighter longitudinal striations were also observed in the front tire marks, and these were considered in the analysis. Once the parking brake was released, striations from the rear leading tire mark were used to calculate longitudinal slip percentages and these values were applied to all tires. When the striation analysis indicated that a driven wheel was free rolling, the wheel was assigned a longitudinal slip percentage of 0.5%, to correspond with the measured rolling resistance of a similar vehicle documented in Reference 10. When tire marks from a non-driven wheel indicated no braking, a longitudinal slip value of 0% was used. In Test 1, the service brakes were not applied after the parking brake was released, so the longitudinal slip percentages were assigned values commensurate with free-rolling wheels. In Test 2, we used the longitudinal slip percentages shown in Figure 7.

Four different methods were used to calculate the deceleration of the vehicle during each of the segments shown in Figures 8 and 9. These methods are summarized in Table 2. The first model, which we have termed the Simple No Braking Model, is similar to a model presented by Daily, Shigamura, and Daily [Reference 11], neglecting rolling resistance and roadway slope. The Simple No Braking Model, as well as the model presented in Reference 11, do not account for braking, and thus the Simple No Braking Model is used here to demonstrate a lower boundary on the speed in a vehicle sideslip angle analysis. Likewise, the Full Lockup Model is presented to demonstrate an upper boundary.

For the analysis in this paper, use of the CRASH model required calculation of the (f_{long}/μ_o) term. To calculate this value for a given segment, we first utilized the striation evidence in the tiremarks to calculate a longitudinal slip percentage, then used the NCB equations and the coefficients listed in Table 1 to determine the proportion of longitudinal

Table 2. The Four Models Used to Analyze Vehicle Speed

1 – Simple No Braking Model	$f_{veh} = \mu_0 \sin \alpha$
2 – Full Lockup Model	$f_{veh} = \mu_0$
3 – BNP/NCB Model	$f_i = \mu_0 \cdot [Q_x(\alpha, s) \cdot cos(\alpha) + Q_y(\alpha, s) \cdot sin(\alpha)]$ $f_{veh} = \frac{1}{W_{total}} \sum_{i=1}^{N} [f_{eff,i} \cdot W_i]$
4 – CRASH Model	$f_i = \mu \sqrt{sin^2\alpha + \left(\frac{f_{long}}{\mu_0}\right)^2 cos^2(\alpha)}$ $f_{veh} = \frac{1}{W_{total}} \sum_{i=1}^{N} [f_{eff,i} \cdot W_i]$

force. In other words, the longitudinal slip was calculated from striation evidence, and used to calculate $Q_X(s)$, which is equivalent to (f_{long}/μ_o) in this application.

Using the deceleration rates calculated with the models in Table 2, speeds at the beginning of each segment were calculated using Equations (10) and (11). These equations yield the speed at the beginning of the segment, given the speed at the end of the segment, the deceleration rate and the segment distance. Equation (10) is in general terms whereas Equation (11) is the common crash reconstruction equation, expressed in units of speed in miles per hour, distance in feet, and acceleration in g's.

$$v_i = \sqrt{{v_{i-1}}^2 + 2ad} \tag{10}$$

$$S_i = \sqrt{{S_{i-1}}^2 + 30fd} \tag{11}$$

For Test #1, our analysis of the vehicle speed began at the end of the tire marks and worked back to the beginning. We chose not to begin the analysis of this test at rest because the VBOX data became erratic during the rollout phase at the end of the test. For Test #2, our analysis began at the vehicle rest position and worked back to the beginning of the tire marks. Figures 11 and 12 depict the results of this analysis. In these graphs, vehicle speed is plotted against distance. The solid black line represents the vehicle speed obtained from the VBOX. The other four curves represent the speeds obtained with the four methods listed in Table 2. As was expected, the no-braking model underestimated the vehicle speed over the entire duration of the test. Similarly, using roadway friction for the deceleration value (full lockup) overestimated the speed. For the two yaw tests analyzed in this study, both the BNP/NCB model and CRASH model yielded acceptable estimates for the vehicle speed.

DISCUSSION

Comparison of the above tire models to full-scale vehicle tests shows that reasonable agreement can be achieved between calculated speeds and actual speeds. Implementation of such a tire model in a spreadsheet has advantages over simulation in that it is often simpler, more straightforward and less time consuming. With a robust tire model, the results can be expected to be similar. However, simulation may account for complexities beyond the scope of the above tire modeling techniques, and may be useful when exploring driver inputs, irregular terrain or time-space relationships.

This paper aimed to explore the accuracy of several tire models for determining the speed of yawing and braking vehicles by comparing the vehicle speeds calculated by the models to vehicle speeds in controlled test conditions. In practice, the crash reconstructionist should consider the uncertainty of inputs to these models for a specific case. For instance, uncertainty in parameters such as the tire-roadway sliding coefficient of friction should be recognized.

The BNP/NCB model and the CRASH model presented above utilize striation analysis to determine braking levels. The striation analysis should not be trivialized, as the

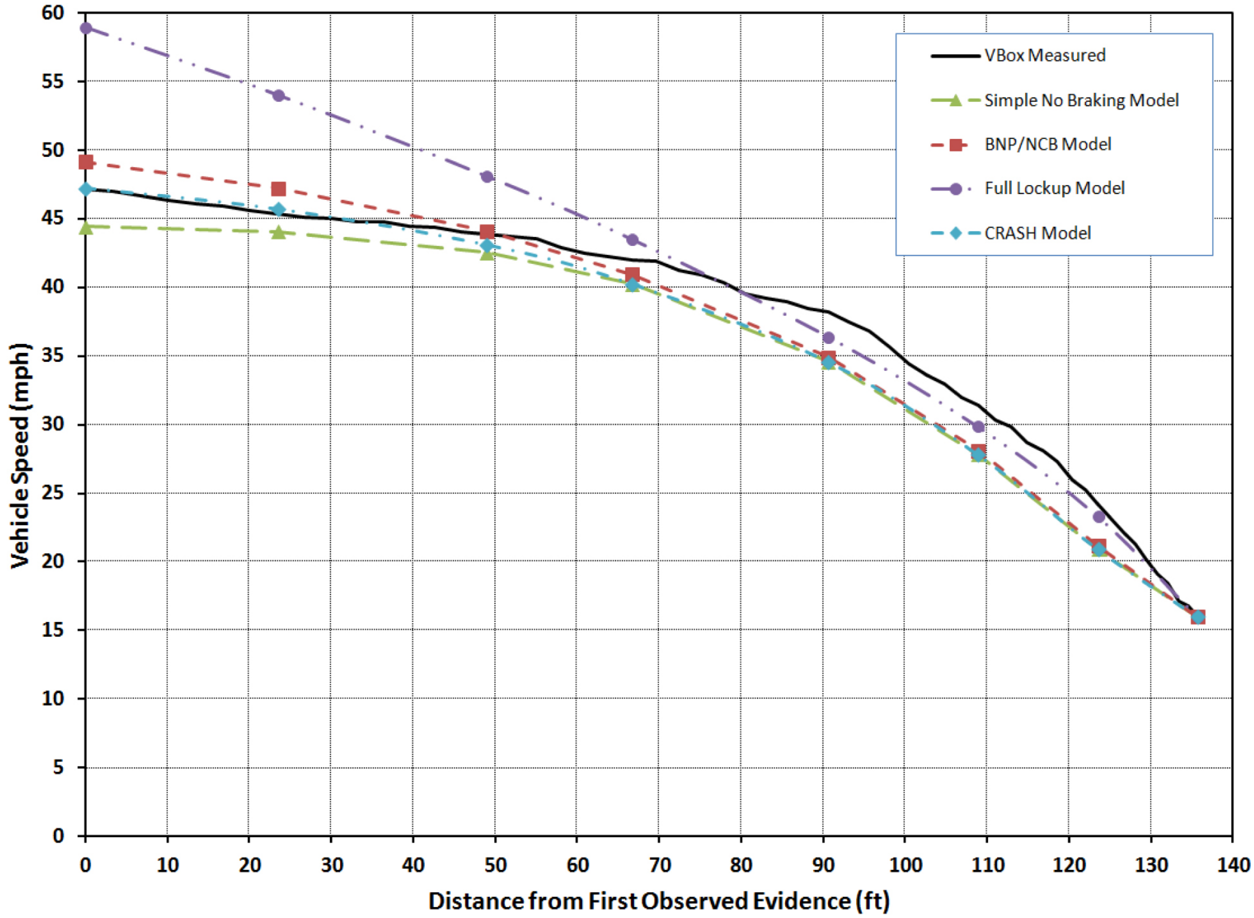

Figure 11. Test 1 Analysis Results

calculated vehicle speeds are sensitive to braking levels, particularly at low vehicle sideslip angles. Absent striations, tire marks can still be used to calculate vehicle sideslip angles, and braking levels can then be varied to provide a speed range.

The tests described in this paper were performed on a four-wheeled passenger vehicle, and thus the conclusions drawn from the tire model comparisons should only be seen as relevant to four-wheeled vehicles. However, it is conceivable that the NCB model and the CRASH model would also be applicable to vehicles with differing number of tires, as long as appropriate BNP coefficients are used for the tire type, and Equation 7 is applied properly to account for all tires. Future testing by the authors may include vehicles with more than four tires.

Although longitudinal and lateral data exist for specific tires, it is unlikely that data for a specific make, model, and size of tire on a subject vehicle will be publicly available, given the immense variety of tires in the marketplace. Thus, the calculations presented utilized representative tire model parameters. Future testing in this area may involve comparison of calculated speeds using generic tire model parameters to those using tire-specific parameters.

Although the BNP/NCB and CRASH models provided reasonable speed estimates when compared to these tests, the models are different. A study of the differences between the models is outside the scope of this paper, but may be the topic of future work.

CONCLUSIONS

The BNP/NCB model yielded satisfactory estimates of the vehicle speed during both tests, despite the use of generic tire model parameters in the BNP equations. This model underestimated the vehicle speeds for the later portions of the test. It slightly overestimated the initial speed for one test and slightly underestimated the initial speed for the other.

The CRASH model yielded satisfactory estimates of the vehicle speed during both tests. Like the BNP/NCB model, the CRASH model underestimated the vehicle speeds for the later portions of the test. The initial vehicle speeds obtained from the CRASH model were nearly identical to the VBOX

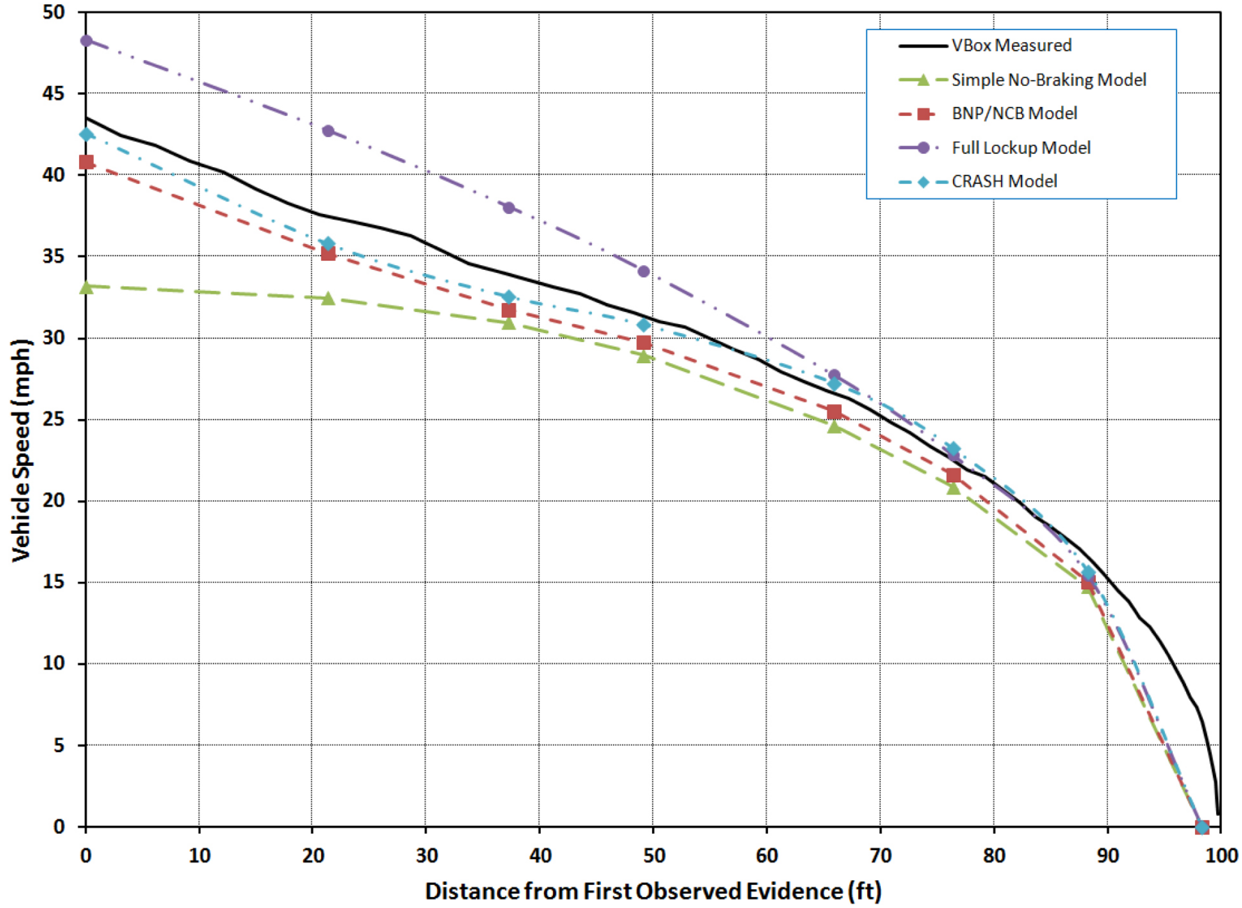

Figure 12. Test 2 Analysis Results

speed for Test 1, and slightly underestimated the speed for Test 2.

The reasonable speed estimates that both the BNP/NCB and CRASH models yielded in this research were achieved with the use of braking levels determined from tire mark striations. Previous research by the authors, which was reported in Reference 9, described the methodology used for this type of analysis. This paper has shown that when implemented, such analysis can yield accurate speed estimates.

REFERENCES

1. Bakker, E., Nyborg, L., and Pacejka, H., "Tyre Modelling for Use in Vehicle Dynamics Studies," SAE Technical Paper 870421, 1987, doi: 10.4271/870421.

2. Brach, R. and Brach, R., "Modeling Combined Braking and Steering Tire Forces," SAE Technical Paper 2000-01-0357, 2000, doi:10.4271/2000-01-0357.

3. Brach, R.M. and Brach, R.M., "Vehicle Accident Analysis and Reconstruction Methods," SAE International, ISBN 978-0768007763, 2005.

4. Brach, Raymond M., Brach, R. Matthew, "Tire Models used in Accident Reconstruction Vehicle Motion Simulation," presented at XVII Europäischen für Unfallforschung und Unfallanalyse (EVU) - Conference, Nice, France, 2008.

5. Brach, R. and Brach, R., "Tire Models for Vehicle Dynamic Simulation and Accident Reconstruction," SAE Technical Paper 2009-01-0102, 2009, doi: 10.4271/2009-01-0102.

6. Martinez, J. and Schlueter, R., "A Primer on the Reconstruction and Presentation of Rollover Accidents," SAE Technical Paper 960647, 1996, doi: 10.4271/960647.

7. Marine, M., Wirth, J., and Thomas, T., "Characteristics of On-Road Rollovers," SAE Technical Paper 1999-01-0122, 1999, doi:10.4271/1999-01-0122.

8. Fricke, Lynn B., Traffic Crash Reconstruction, Second Edition, Northwestern University Center for Public Safety, 2010.

9. Beauchamp, G., Hessel, D., Rose, N., Fenton, S. et al., "Determining Vehicle Steering and Braking from Yaw Mark Striations," *SAE Int. J. Passeng. Cars - Mech. Syst.* 2(1): 291-307, 2009, doi:10.4271/2009-01-0092.

10. Cliff, William E., Bowler, James J., "The Measured Rolling Resistance of Vehicles for Accident Reconstruction," Society of Automotive Engineers Paper Number 980368, 1998.

11. Daily, John, Shigemura, Nathan, Daily, Jeremy, "Fundamentals of Traffic Crash Reconstruction," Institute of Police Technology and Management, ISBN 1884566634, 2006.

CONTACT

Neal Carter
Kineticorp, LLC
6070 Greenwood Plaza Blvd., Suite 200
Greenwood Village, Colorado 80111
(303) 733-1888
ncarter@kineticorp.com
www.kineticorp.com

ACKNOWLEDGEMENTS

The authors would like to thank Toby Terpstra of Kineticorp, LLC for producing graphics used in this paper.

The Engineering Meetings Board has approved this paper for publication. It has successfully completed SAE's peer review process under the supervision of the session organizer. This process requires a minimum of three (3) reviews by industry experts.

All rights reserved. No part of this publication may be reproduced, stored in a retrieval system, or transmitted, in any form or by any means, electronic, mechanical, photocopying, recording, or otherwise, without the prior written permission of SAE.

ISSN 0148-7191

Positions and opinions advanced in this paper are those of the author(s) and not necessarily those of SAE. The author is solely responsible for the content of the paper.

SAE Customer Service:
Tel: 877-606-7323 (inside USA and Canada)
Tel: 724-776-4970 (outside USA)
Fax: 724-776-0790
Email: CustomerService@sae.org
SAE Web Address: http://www.sae.org
Printed in USA

SAE International®